

# A FREE STREAMLINE THEORY FOR TWO-DIMENSIONAL FULLY CAVITATED HYDROFOILS\*

BY T. YAO-TSU WU

**I. Introduction.** The problem of cavity flows received attention early in the development of hydrodynamics because of its occurrence in high speed motion of solid bodies in water. Many previous works in this field were mainly concerned with the calculation of drag in a cavitating flow. The lifting problem with a cavity (or wake) arose later in the applications of water pumps, marine propellers, stalling airfoils, and hydrofoil crafts. Although several formulations of the problem of lift in cavity flows have been pointed out before (1-3), these theories have not yet been developed to yield general results in explicit form so that a unified discussion can be made.

The problems of cavitating flow with finite cavity demand an extension of the classical Helmholtz free boundary theory for which the cavity is infinite in extent. For this purpose, several self-consistent models have been introduced, all aiming to account for the cavity base pressure which is in general always less than the free stream pressure. In the Helmholtz-Kirchhoff flow these two pressures are assumed equal.

Of all these existing models, three significant ones may be mentioned here. The first representation of a finite cavity was proposed by Riabouchinsky (4) in which the finite cavity is obtained by introducing an "image" obstacle downstream of the real body. A different representation in which a reentrant jet is postulated was suggested by Prandtl, Wagner, and was later considered by Kreisel (5) and was further extended by Gilbarg and Serrin (3). Another representation of a free streamline flow with the base pressure different from the free stream pressure was proposed recently by Roshko (6). In this model the base pressure in the wake (or cavity) near the body can take any assigned value. From a certain point in the wake, which can be determined from the theory, the flow downstream is supposed to be dissipated in such a way that the pressure increases gradually from the assigned value to that of the free stream in a strip parallel to the free stream. Apparently this model was also considered independently by Eppler (7) in some generality. Other alternatives to these models have also been proposed (8), but they do not differ so basically from the above three models that they need to be mentioned here specifically. The mathematical solutions to the problem of flow past a flat plate set normal to the stream have been carried out for these three models (9, 6). All the theories are found to give essentially the same results over the practical range of the wake underpressure. That such agreement is to be expected can be indicated, without the detailed solutions for the various models, from consideration of their underlying physical significance, as will be discussed in the next section.

\* This study was supported by the U. S. Navy, Office of Naval Research, under Contract N6onr-24420 (NR 062-059). Reproduction in whole or in part is permitted for any purpose of the U. S. Government.

In the present work the free streamline theory is extended and applied to the lifting problem for two-dimensional hydrofoils with a fully cavitating wake. The analysis is carried out by using the Roshko model to approximate the wake far downstream. The reason for using this model is mainly because of its mathematical simplicity as compared with the Riabouchinsky model, or the reentrant jet model. In fact, it can be verified that these different models all yield practically the same result, as in the pure drag case; the deviation from the results of one model to another is not appreciable up to second order small quantities. The mathematical considerations here, as in the classical theory, depend on the conformal mapping of the complex velocity plane into the plane of complex potential. By using a generalization of Levi-Civita's method for curved barriers in cavity flows, the flow problem for curved hydrofoils is finally reduced to a nonlinear boundary value problem for an analytic function defined in the upper half of a unit circle to which the Schwarz's principle of reflection can be applied. The problem is then solved by using the expansion of this analytic function inside the unit circle together with the boundary conditions in the physical plane. In order to avoid the difficulty in determining the separation point of the free streamline from a hydrofoil with blunt nose, the hydrofoils investigated here are those with sharp leading and trailing edges which are assumed to be the separation points. Except for this limitation, the present nonlinear theory is applicable to hydrofoils of any geometric profile, operating at any cavitation number, and for almost all angles of attack as long as the wake has a fully cavitating configuration.

As two typical examples, the problem is solved in explicit form for the circular arc and the flat plate for which the various flow quantities are expressed by simple formulas. From the final result the various effects, such as that of cavitation number, camber of the profile and the attack angle, are discussed in detail. It is also shown that the present theory is in good agreement with the experiment.

**II. Remarks on Models in Free Streamline Theory.** The total force (drag and lift for two-dimensional flows) exerted by the fluid on a solid body may of course be expressed as an integral of the local force, which consists of both the pressure and viscous stresses over the surface of the solid. However, it is also possible to express the total force in terms of integrals over surfaces at a distance from the body by applying the momentum theory. In the case of the real fluid flow past a bluff body, experimental observations indicate that the discontinuous surfaces in the flow, or free streamlines, are actually thin shear layers, into which the vorticity is fed from the boundary layer in front of the separation point. The shear layers in general do not continue smoothly far downstream, but roll up to form vortices, alternately on each side with a certain frequency. These vortices diffuse rapidly and are eventually dissipated in the wake. With a constant upstream velocity, the wake flow is thus only stationary in the mean. Because of this complicated wake flow, it seems rather fruitless to apply the momentum theory which requires a detailed consideration of the free streamlines

at infinity. A more realistic way to formulate the problem is thus to obtain a solution which is accurate near the body by taking appropriate consideration of the cavity pressure. It is physically plausible that the detailed structure of the wake far downstream has indeed negligible influence upon the flow field near the body. Consequently, one may represent the dissipative wake flow by an equivalent model of potential flow, if properly chosen.

The general character of cavity flows depends on the value of the cavitation number  $\sigma$  which is defined by

$$\sigma = (P - p_\sigma) / (\frac{1}{2}\rho U^2) \quad (2.1)$$

where  $P$  denotes the pressure of the undisturbed free stream,  $U$  is its relative velocity,  $\rho$  is the fluid density, and  $p_\sigma$  is the pressure of the vapor or gas in the cavity. Physical cavities usually have finite length and positive cavitation number ( $\sigma > 0$ , or  $p_\sigma < P$ ). Some mathematical formulations have been suggested previously to investigate the possibility for obtaining the solution of steady cavity flows of ideal fluid satisfying the following conditions:

- (i) the cavitation number is greater than zero,  $\sigma > 0$ , or  $p_\sigma < P$ ;
- (ii) the cavity pressure is uniform throughout the cavity;
- (iii) the pressure of the fluid is nowhere less than the cavity pressure;
- (iv) the pressure is continuous across the cavity boundary.

The first two conditions are imposed because of their physical reality ( $\sigma = 0$  case is physically unreal). The third condition follows from the potential flow theory that the velocity cannot have a maximum in the interior of the flow field. The last condition states that the interface between two phases of fluid cannot withstand any pressure jump. It then follows from (ii) that the free streamlines are surfaces of constant velocity; also, (iii) always implies that the cavity boundary is convex towards the interior flow. Application of Bernoulli's equation with condition (iii) shows that the velocity is maximum on the cavity boundary. It should be noted that these conditions differ only in (i) from the classical theory, for which  $\sigma = 0$  (or  $p_\sigma = P$ ), corresponding to an infinitely long cavity. If the flow is restricted to be everywhere potential flow, then the cavity cannot have finite length for  $\sigma \geq 0$ . For if the cavity were to close up at the rear end by itself, then the free streamlines from two sides of the body should meet either at a stagnation point from opposite directions or with a cusp in the downstream direction. The first conjecture contradicts (ii), while the second alternative violates (iii). Though the streamlines may reverse in direction and form a reentrant jet, as often observed, the jet cannot terminate in the physical plane. The above argument indicates the need of models of potential flow to represent the dissipative wake downstream if the formulation of the problem is to be retained within the scope of potential theory.

Now the problem of flow past a two-dimensional flat plate set normal to the stream, forming a finite cavity, shall be reviewed to exhibit the characteristics of these models. In the model of Riabouchinsky, an image plate  $A'$  (see Fig. 1a) is put downstream of the real plate  $A$ . The free streamlines run from  $A$  to  $A'$  and the flow field is assumed irrotational everywhere. The total force on the pair

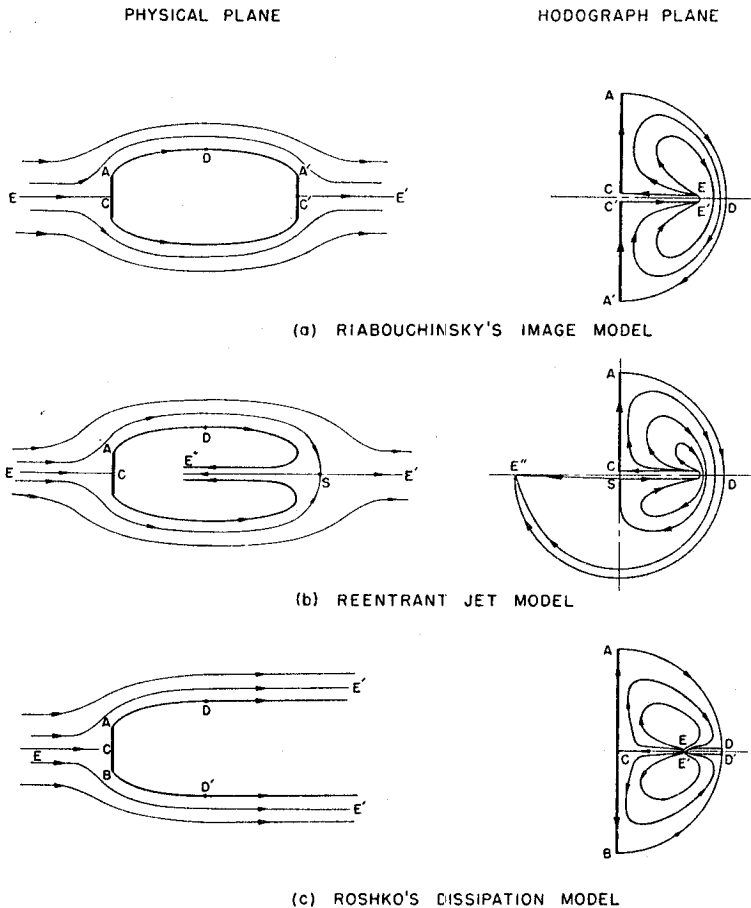


FIG. 1. Flows in the physical and hodograph plane for the various models. Note the resemblance of the streamlines in the hodograph planes near the plate AC.

of plates then vanishes, but the calculation of the drag on  $A$  alone yields the following approximate expression for the drag coefficient:

$$C_D(\sigma) \cong \{1 + \sigma + [8(\pi + 4)]^{-1}\sigma^2\} C_D(0) \cong (1 + \sigma) C_D(0) \quad (2.2)$$

where  $C_D(0) = 2\pi/(4 + \pi) = 0.88$  is the classical Helmholtz solution for  $\sigma = 0$ . The physical significance of the image plate can perhaps be justified by the following argument. In a coordinate system where the fluid at infinity is at rest, the force holding  $A'$  does an amount of negative work, equal to  $W = -DU$ , where  $D$  is the drag on  $A$  and  $U$  is the speed of the traveling plates. The coefficient of work defined by  $C_w = W/(\frac{1}{2}\rho U^3 l)$ , where  $l$  is the plate width, then equals  $-C_D$ . Now if the wake is approximated by a vortex street and  $C_D$  be calculated from the vortex energy shed into the wake, the result is (see Ref. 10, p. 557)

$$C_D = \frac{a}{l} \left[ 1.59 \frac{U_s}{U} - 0.63 \left( \frac{U_s}{U} \right)^2 \right] \quad (2.3)$$

where  $a$  is the spacing between consecutive vortices in the same row and  $U_s$  is the receding velocity of the vortices relative to the undisturbed flow. If the air is taken to be the fluid medium (because of more data available in this case), the measured underpressure (11) corresponds to  $\sigma = 1.2$  for which Eq. (2.2) gives  $C_D = 1.93$ . For the same flow, Heisenberg (10) showed, by using some representative experimental values, that Eq. (2.3) yields  $C_D = 1.82$ . Thus, the work done by the image plate, even though it does not exist in reality, provides a good representation of the energy shed to the wake, which should be removed from the flow if the flow is assumed to be potential. It should be noted that the result Eq. (2.2) together with the assumed flow configuration actually imposes on  $A'$  a certain restriction that  $A'$  must be of the same size as  $A$ . Now when asymmetric bodies, such as the lifting plate, are considered, a question arises whether the image body should be in symmetry with respect to a plane normal to the stream or only to a point in the cavity. In the former case, the physical reasoning suggests that a circulation around the cavity is necessary to generate a total lift on the pair of bodies; while in the later case, the potential is continuous everywhere in the fluid. A clarification of this vague point certainly seems necessary.

In the reentrant jet model, the free streamlines reverse direction at the rear of the cavity to form a jet which flows upstream in the cavity (see Fig. 1b) and is supposed not to impinge on the real body but is removed mathematically by allowing it to flow on a second Riemann sheet in the physical plane to infinity. Thus, in the original physical plane, the point infinity acts like a doublet plus a source, while the jet represents a sink. Physically, the jet momentum carried away from the first sheet is then closely associated with the energy dissipated in the wake. For even though the jet can usually be observed, it is rather weakened by the turbulent mixing, at least its observed width is much smaller than its theoretical value. For the flat plate flow, the theory yields for  $C_D(\sigma)$  the same formula as Eq. (2.2), the jet width is  $0.22(1 + \sigma/4)$  of the plate width. In the lifting problems, it can be shown from consideration of momentum that the jet will turn in direction and eventually flow towards the downstream on the second sheet for small enough attack angles.

In Roshko's dissipation model, the flow past a bluff body is considered in two parts. Near the body it is described by the free streamline theory to allow a possible adjustment of the underpressure. The flow farther downstream is described by an equivalent potential flow so that its pressure increases continuously to the free stream value as it approaches infinity in a strip parallel to the free stream (see Fig. 1c). In this manner, the actual dissipative wake flow is represented; the detailed mechanism according to which the flow is dissipated is immaterial. Thus, it can be seen that this model is actually closer to the physical fact than the other models for the air flow past bluff bodies. However, this model applies equally well to cavity flows if the wake in front of the dissipation range is considered to be the front half of the cavity. By using this theory, the solution of  $C_D(\sigma)$  on the flat plate differs from the previous two solutions, Eq. (2.2), only slightly by a term of  $O(\sigma^2)$ . Moreover, for the lifting problems, the assumption that the dissipative wake is parallel to the free stream is still physically sound and hence needs no further modification.

To summarize, all these models have one essential feature in common: they are aimed to give a satisfactory description of the flow near the body by making possible an adjustment of the base pressure and thereby removing a serious limitation in the classical theory. For this reason, it should not be expected that these solutions of the flow field shall describe the wake far downstream. The freedom of adjusting the base pressure, therefore, yields a family of solutions containing one parameter which can be expressed in terms of  $\sigma$ . For pure drag problems, the agreement of these theories in that they all yield the result Eq. (2.2) can be explained also from consideration of the hodograph involved (see Fig. 1 and Refs. 12, 13). However, it should be pointed out that for lifting problems the linear relation in  $\sigma$  for  $C_L$  and  $C_D$  such as given by Eq. (2.2) becomes invalid for moderate and small attack angles as will be shown by the present analysis. Consequently, the problem of calculating  $C_L(\sigma)$  and  $C_D(\sigma)$  cannot be reduced to the calculation of  $C_L(0)$  and  $C_D(0)$  for a given geometric configuration, as is usually done in pure drag problems.

With respect to the mathematical details involved in the analysis, these models differ in simplicity to some extent, especially for the lifting case. In Riabouchinsky's theory, some numerical integration containing elliptical integrals are required. Although the results obtained by using the reentrant jet model are expressible in terms of elementary functions, the Roshko model is still simpler in many respects.

**III. Formulation of the Problem.** The free streamline theory is applied here to investigate the steady, two-dimensional flow at a given attack angle  $\alpha$  past a hydrofoil with a fully cavitating wake. The leading and trailing edges of the hydrofoil are assumed to be sharp and the flow configurations concerned are such that free streamlines separate from the hydrofoil at these sharp edges, but otherwise the wetted side of the hydrofoil may have any continuous profile. After the cavity is fully developed, the thickness of the hydrofoil has no effect on the flow and, therefore, the hydrofoil will be assumed to be of zero thickness. The Roshko model (see previous sections) will be used to approximate the wake far downstream. The flow in the physical space (or  $z$ -plane, where  $z = x + iy$  with  $x$  parallel to the free stream) is shown in Fig. 2. Outside the wake the flow is assumed to be everywhere irrotational. Thus, from the complex potential

$$W(z) = \varphi(x, y) + i\psi(x, y),$$

the complex velocity  $w$  can be derived as

$$w(z) = dW/dz = u - iv = qe^{-i\theta},$$

where  $q$ ,  $\theta$  are the magnitude and direction of the velocity field. Here, the velocity at separation is normalized to  $q = 1$ , and remains at this value along the free streamlines until the latter reach points  $D$  and  $D'$  where  $\theta = 0$ . Downstream of these two points, the free streamlines keep parallel to the free stream on  $DE'$  and  $D'E'$  along which  $q$  decreases from unity back to the free stream value  $U$ . In order that the cavitation number of the flow be  $\sigma$  (see Eq. (2.1) for its definition)

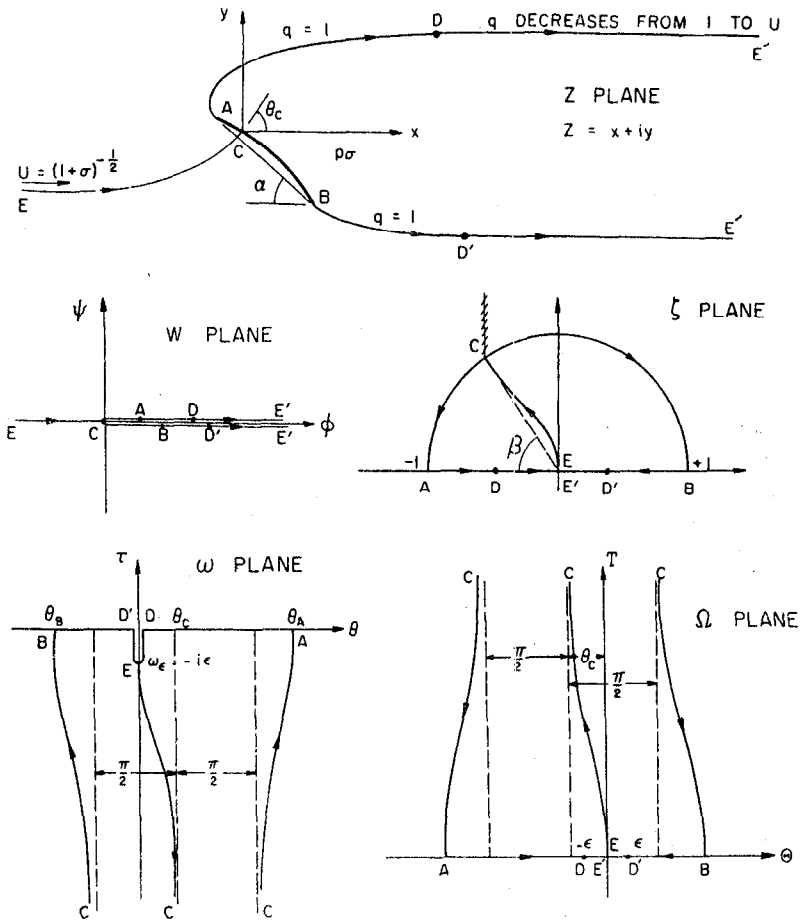


FIG. 2

with  $q = 1$  on  $AD$  and  $BD'$ ,  $U$  takes the value  $(1 + \sigma)^{-\frac{1}{2}}$ , as can be shown by applying Bernoulli's equation

$$p + \frac{1}{2}\rho q^2 = P + \frac{1}{2}\rho U^2.$$

The mathematical problem can be treated by finding the conformal transformation which maps the  $W$ -plane into the  $w$ -plane. From this relation the physical plane can be deduced by an integration

$$z = \int dW/w$$

We introduce to  $W$  a transformation in  $\zeta$  which is given by

$$\sqrt{W} = -b[\cos \beta + \frac{1}{2}(\zeta + \zeta^{-1})] \tag{3.1}$$

where

$$b = \frac{1}{2}(b_1 + b_2), \quad \cos \beta = (b_2 - b_1)/(b_1 + b_2),$$

and  $b_1$  and  $b_2$  are two positive quantities defined by the potential at  $A$  and  $B$

$$W_A = b_1^2, \quad W_B = b_2^2 e^{2\pi i}.$$

This transformation maps the entire flow in the  $W$ -plane into the interior of the upper semi-circle of unit radius in the  $\zeta$ -plane. The barrier  $ACB$  corresponds to the semi-circle  $|\zeta| = 1, 0 \leq \arg \zeta \leq \pi$ , and the free streamlines  $ADE'$  and  $BD'E'$  map on to the two halves of the diameter along the real axis. The approaching streamline  $EC$  leaves  $\zeta = 0$  perpendicular to the real axis and approaches  $C$  along the direction  $\arg \zeta = \pi - \beta$ .

Because of the way the nonlinear boundary conditions are specified in the  $z$ -plane (that is, with  $\theta$  described on the barrier and  $q$  given on the free streamlines), we introduce the variable

$$\omega = i \log w = \theta + i \log q \equiv \theta + i\tau.$$

The flow in the  $\omega$ -plane is sketched in Fig. 2. The jump in the real component  $\theta$  of  $\omega$  at  $C$ , where  $\tau = -\infty$ , follows from the fact that the two branches of the streamlines at the stagnation point  $C$  in the  $z$ -plane are orthogonal. The notch  $DED'$  in the  $\omega$ -plane results from the assumption introduced in this model. At  $E$ ,  $\omega_E = -i\varepsilon$  where  $\varepsilon = \frac{1}{2} \log(1 + \sigma)$ . This notch can be removed by the transformation

$$\Omega = -\sqrt{\omega^2 + \varepsilon^2}, \quad \varepsilon = \frac{1}{2} \log(1 + \sigma). \tag{3.2}$$

It should be noted that the present case ( $\sigma > 0$ ) differs from the classical theory ( $\sigma = 0$ ) only by the last transformation. When  $\sigma = 0$ ,  $\Omega$  and  $-\omega$  become identical and the problem reduces to the classical Levi-Civita problem.

It follows from the jump condition of  $\Omega(\zeta)$  at  $\zeta_c = e^{i(\pi-\beta)}$  that the analytic function  $\Omega(\zeta)$  has a logarithmic singularity at  $\zeta_c$  and is regular elsewhere within the semi-circle. Moreover, we note that  $\Omega(\zeta)$  is real for real  $\zeta$ , and therefore the function  $\Omega(\zeta)$  can be continued analytically over the lower half of the unit circle by applying Schwarz's principle of symmetry. More precisely, since  $\Omega(0) = 0$ , we may express the function  $\Omega(\zeta)$  by

$$\Omega(\zeta) = i \log [(1 + \zeta e^{-i\beta}) / (1 + \zeta e^{i\beta})] + \sum_{n=1}^{\infty} A_n \zeta^n. \tag{3.3}$$

The first term on the right-hand side represents the singular part of  $\Omega(\zeta)$  while the series denotes the expansion of an analytic function, regular and hence convergent, in and on the unit circle. The coefficients,  $A_n$ 's, are real and can be determined in principle from the geometry of the barrier  $ACB$  (see Sec. 4). Near the origin, we have

$$\Omega(\zeta) = \sum_{n=1}^{\infty} \left[ (-1)^{n+1} \frac{2}{n} \sin n\beta + A_n \right] \zeta^n \equiv \sum_{n=1}^{\infty} a_n \zeta^n, \quad (|\zeta| < 1). \tag{3.4}$$

On the barrier, where  $\zeta = e^{i\eta}, 0 \leq \eta \leq \pi$ , we have

$$T(\eta) = \text{Im } \Omega = \frac{1}{2} \log \frac{1 + \cos(\eta - \beta)}{1 + \cos(\eta + \beta)} + \sum_{n=1}^{\infty} A_n \sin n\eta; \tag{3.5a}$$



$$\Theta(\eta) = \text{Rl } \Omega = \beta_0 + \beta + \sum_{n=1}^{\infty} A_n \cos n\eta; \quad (3.5b)$$

where  $\beta_0 = 0$  for  $0 \leq \eta < (\pi - \beta)$  and  $\beta_0 = -\pi$  for  $(\pi - \beta) < \eta \leq \pi$ . Now from the definition of  $\omega$  and the expression of  $W$  in terms of  $\zeta$ , (3.1), the physical plane  $z(\zeta)$  can be obtained by integrating

$$dz = e^{i\omega} dW = \frac{b^2}{2} \exp \{-i(\Omega^2 - \varepsilon^2)^{\frac{1}{2}}\} \left( \zeta + \frac{1}{\zeta} + 2 \cos \beta \right) \left( \zeta - \frac{1}{\zeta} \right) \frac{d\zeta}{\zeta} \quad (3.6)$$

which, in particular, reduces on the wetted wall,  $\zeta = e^{i\eta}$ , to

$$z = 2b^2 \int_{\eta}^{\pi-\beta} e^{-i(\Omega^2 - \varepsilon^2)^{\frac{1}{2}}} (\cos \eta + \cos \beta) \sin \eta \, d\eta. \quad (3.7)$$

The arc length of the barrier along  $CA$  or  $CB$  can be determined from

$$s = \int_{\eta}^{\pi-\beta} \left| \frac{dz}{d\eta} \right| d\eta = 2b^2 \int_{\eta}^{\pi-\beta} e^{-\tau(\eta)} (\cos \eta + \cos \beta) \sin \eta \, d\eta; \quad (3.8)$$

and the total length of the wetted wall is then

$$S = 2b^2 \int_0^{\pi} e^{-\tau(\eta)} |\cos \eta + \cos \beta| \sin \eta \, d\eta \quad (3.9)$$

where  $\tau = \text{Im } \omega = -\text{Im} (\Omega^2 - \varepsilon^2)^{\frac{1}{2}}$ . The radius of curvature of the barrier is given by

$$R = \frac{ds}{d\theta} = 2b^2 e^{-\tau(\eta)} |\cos \eta + \cos \beta| \sin \eta \frac{d\eta}{d\theta}. \quad (3.10)$$

If  $X$  denotes the drag,  $Y$ , the lift, then it can be shown that the force is given by (e.g. Ref. 14, p. 305)

$$\begin{aligned} X + iY &= -\frac{i\rho}{2} \oint e^{i\omega} \frac{dW}{d\zeta} d\zeta \\ &= -\frac{i\rho b^2}{4} \oint \exp \{-i(\Omega^2 - \varepsilon^2)^{\frac{1}{2}}\} \left( \zeta + \frac{1}{\zeta} + 2 \cos \beta \right) \left( \zeta - \frac{1}{\zeta} \right) \frac{d\zeta}{\zeta} \end{aligned} \quad (3.11)$$

where the contour for the integral is  $|\zeta| = 1$ . Likewise the moment  $M$  of the force about the stagnation point  $C$ , positive in the sense of nose-down, is found to be (14)

$$M = \frac{\rho}{2} \text{Rl} \int_{(BCA)} [e^{-i\omega(\zeta)} - e^{-i\omega(\bar{\zeta})}] z \frac{dW}{d\zeta} d\zeta; \quad (3.12)$$

the integration is taken around the semi-circle  $BCA$  in the  $\zeta$ -plane. The above integral cannot be reduced to one on a closed contour, and, therefore, must be evaluated separately.

The above formulas are merely formal representations of various physical quantities. The magnification factor  $b$  for the physical plane may be eliminated from Eqs. (3.8)–(3.10). If the boundary value  $R(s)$  is applied to these two resulting equations, an identity containing all the coefficients  $A_n$  in the parameter

of  $\eta$  can be obtained. From this identity the coefficients  $A_n$  can, at least in principle, be determined. The factor  $b$  can then be expressed by (3.9) in terms of the wall length  $S$ , and in turn,  $X, Y, M$  can be calculated from Eqs. (3.11), (3.12). In practice, however, to determine the coefficients  $A_n$  from the identity would necessitate some expansion of the functions of  $\eta$  involved in the identity into series. This procedure leads to infinitely many transcendental equations in infinitely many unknowns. In order to obtain the general result in explicit form with sufficient accuracy, the analysis is carried out by replacing the expansion in Eq. (3.3) by the three leading terms only, that is,

$$\Omega(\zeta) = i \log [(1 + \zeta e^{-i\beta}) / (1 + \zeta e^{i\beta})] + A_1 \zeta + A_2 \zeta^2 + A_3 \zeta^3. \quad (3.13)$$

If two particular points are suitably chosen on the arc  $ACB$  at which the boundary values of  $R$  and  $\theta$  are applied, we get four transcendental equations from which the four unknowns,  $\beta, A_1, A_2,$  and  $A_3$  can be determined, expressible in terms of the cavitation number  $\sigma$ , the attack angle  $\alpha$ , and the profile shape. The rest of the physical quantities can then be calculated as shown below.

a. *Lift and Drag.* In the integral representing the force, given by Eq. (3.11), the integrand has inside the contour  $|\zeta| = 1$  only one pole at  $\zeta = 0$ , but has, in addition, two branch points at  $\Omega = \pm \epsilon$ . Besides, the function  $\Omega(\zeta)$  in the integrand has on the contour a logarithmic singularity at  $C$  and its conjugate point in the  $\zeta$ -plane. Thus, if a branch cut is introduced from  $D$  to  $D'$  along the real axis in both the  $\zeta$ - and  $\Omega$ -planes and two other branch cuts from  $C$  to its conjugate point outside of the unit circle in  $\zeta$ -plane (see Fig. 2), the integrand is then one valued inside and on the contour in the cut plane. In practical applications, the values of the cavitation number  $\sigma$  usually fall in the range  $0 < \sigma < 1$ , corresponding to  $0 < \epsilon^2 < 0.123$ , which can therefore be considered small. Moreover, the modulus  $|\Omega|$  is always greater than  $\epsilon$  on the contour. Therefore, the exponential function in Eq. (3.11) can be expanded in terms of the small quantity  $\epsilon^2$ ,

$$\exp \{-i(\Omega^2 - \epsilon^2)^{1/2}\} = \exp \left\{ -i\Omega + \frac{i\epsilon^2}{2\Omega} + O(\epsilon^4) \right\} = e^{-i\Omega} \left( 1 + \frac{i\epsilon^2}{2\Omega} + O(\epsilon^4) \right). \quad (3.14)$$

It can be verified that the term of  $O(\epsilon^4)$  has indeed negligible value and thus may be omitted. Upon substitution of Eqs. (3.13), (3.14) into (3.11), the resulting integral is of the form to which the theorem of residues can readily be applied. From the residue of the integrand at  $\zeta = 0$ , one obtains the following result:

$$X = \pi \rho b^2 \left( 1 + \frac{\epsilon^2}{6} \right) (\sin \beta + A_1/2)^2, \quad (3.15)$$

$$Y = \pi \rho b^2 (1 + \epsilon^2/4) \left\{ (\sin \beta \cos \beta + A_1 \cos \beta + A_2/2) + \frac{\epsilon^2}{4} \cos \beta \left( \sin \beta + \frac{A_1}{2} \right)^{-4} \left[ \left( \sin \beta + \frac{A_1}{2} \right)^3 + \sin \beta \left( \sin \beta + \frac{A_1}{4} \right) \left( \frac{A_1}{2} + \frac{5}{4} A_2 + A_3 \right) \right] \right\}. \quad (3.16)$$

In Eq. (3.16) the quadratic terms in  $A_2$  and  $A_3$  are omitted because their contribution is negligible. It should be remarked here that Eq. (3.16) is valid when the denominator,  $(\sin \beta + A_1/2)$ , of the last term is greater than zero, implying further that the drag  $X$  is always positive definite. For, if this quantity vanishes, then the expansion of  $\Omega(\zeta)$  near  $\zeta = 0$  (see Eq. (3.4)) starts with  $\zeta^2$  and hence the mapping fails to be conformal at  $\zeta = 0$ , indicating that the flow configuration is basically different from what is being considered. If this quantity becomes negative, then the function  $\Omega(\zeta)$  changes its branch, implying physically that the cavity shifts sides on the barrier so that different boundary conditions should be used. With the modified boundary conditions, the present formulation, however, would remain valid.

The factor  $b^2$  in the above equation can be expressed in terms of the arc length  $S$  of the barrier. To evaluate the integral representing  $S$  in (3.9), we first expand  $\exp(-\tau)$  in a way similar to that in (3.14),

$$e^{-\tau(\eta)} = \exp \{ \text{Im} (\Omega^2 - \varepsilon^2)^{\frac{1}{2}} \} = e^{\tau(\eta)} \left[ 1 + \frac{\varepsilon^2}{2} \frac{T}{\Theta^2 + T^2} + 0(\varepsilon^4) \right] \quad (3.17)$$

where  $\Omega(e^{i\eta}) = \Theta(\eta) + iT(\eta)$ , and  $\Theta, T$  are given in Eq. (3.5) with  $A_4 = A_5 = \dots = 0$ . Substituting Eq. (3.17) into (3.9), we obtain

$$S = 2b^2 \int_0^\pi \left( 1 + \frac{\varepsilon^2}{2} \frac{T}{\Theta^2 + T^2} \right) \left[ 1 + \sum_{n=1}^3 A_n \sin n\eta \right] [1 + \cos(\eta - \beta)] \sin \eta \, d\eta$$

in which the higher order terms of  $A_n$  are neglected. The function  $T/(\Theta^2 + T^2)$  is positive and, as can be shown, is bounded above by a constant of order unity, which depends on the value of  $\Theta$  at  $B$  but is independent of  $\varepsilon$ . Hence the contribution from the term of  $0(\varepsilon^2)$  is very small relative to the first order term. Carrying out the integration, we finally obtain

$$Sb^{-2} \equiv J = 4 + \pi \sin \beta + A_1 \left( \pi + \frac{8}{3} \sin \beta \right) + \frac{\pi}{2} A_2 \cos \beta - \frac{8}{15} A_3 \sin \beta. \quad (3.18)$$

For a flat plate set at an angle  $\alpha$ , moving at the idealized limiting condition  $\sigma = 0$  ( $\varepsilon = 0$ ), the coefficients  $A$ 's all vanish, as required by the condition of conformal mapping, and  $\beta = \alpha$  (see Eq. (3.5b)), then Eqs. (3.15), (3.16) and (3.18) reduce to the classical result for an oblique lamina (see Ref. 15, p. 102).

b. *Moment of Force; Stagnation Point; Center of Pressure.* Applying a similar approximation, as described in Eq. (3.17), to Eqs. (3.12) and (3.7), and further neglecting  $A_3$ , we obtain

$$M = 2b^2 \rho \text{Rl} \int_0^\pi \exp \{ i(\beta + A_1 \cos \eta + A_2 \cos 2\eta) \} \\ \cdot [\sin \beta + (A_1 + 2A_2 \cos \eta)(1 + \cos \beta \cos \eta)] (\sin^2 \eta) z(\eta) \, d\eta$$

where

$$z(\eta) = 2b^2 e^{-i\beta} \int_\eta^{\pi-\beta} [1 - iA_1 e^{i\eta} - iA_2 e^{2i\eta}] [1 + \cos(\eta - \beta)] \sin \eta \, d\eta.$$

We then substitute the integral for  $z(\eta)$  into the former expression, decompose accordingly the interval into two parts:  $0 \leq \eta \leq \pi - \beta$  and  $\pi - \beta \leq \eta \leq \pi$ , and then interchange the order of integration so that the limits of integration further simplify the involved manipulation. After some tedious integrations, which are otherwise straightforward, we finally obtain

$$\begin{aligned}
 M/(2\pi\rho b^4) \equiv K = C_1 & \left\{ \cos \beta \left[ \frac{5}{8} + \sin^2 \beta + A_1 \left( \frac{7}{6} \sin \beta + \frac{2}{3} \sin^3 \beta - \frac{32}{45\pi} \right) \right] \right. \\
 & + \frac{C_1}{2} \left( \frac{\pi}{2} - \beta \right) - A_2 \left( \frac{3}{16} \sin \beta + \frac{1}{12} \sin^3 \beta - \sin^5 \beta + \frac{64}{45\pi} \right) \left. \right\} \\
 & + C_2 \left( 1 + A_1 + \frac{A_2}{4} \cos \beta \right) \left( 1 + \frac{128}{45\pi} \sin \beta \right) \\
 & + \frac{A_2}{16} \cos \beta \left( 1 + \frac{5}{6} A_1 \right), \tag{3.19}
 \end{aligned}$$

where  $b^2$  is given by Eq. (3.18) and

$$C_1 = \sin \beta + A_1 + \frac{A_2}{2} \cos \beta; \quad C_2 = \frac{1}{4}(A_1 \cos \beta + 2A_2).$$

If a profile symmetrical with respect to the central chord is set with its chord normal to the free stream, then  $\beta = \pi/2$  due to symmetry (see Fig. 2). Furthermore,  $A_2$  should vanish because in this case  $\Omega(\zeta)$  is necessarily an odd function of  $\zeta$  (see Eq. (3.13)). It then follows from Eq. (3.19) that the moment  $M$  about the stagnation point, which is now at the central chord, vanishes as it should be expected.

Because of the indefinite location of the stagnation point, the moment of force is usually calculated or measured referring to a fixed point. Hence, we derive here the moment  $M_0$  about the leading edge. This further requires the calculation of the position of stagnation point. Denote the distance along the wall from the stagnation point to the leading edge by  $S_0$ ; then  $S_0$  can be calculated from Eq. (3.8) by letting the lower limit  $\eta = \pi$ . Proceeding in a manner similar to that described for the equation previous to (3.18), we obtain

$$S_0 \cong 2b^2 \int_0^\beta (1 + A_1 \sin \theta - A_2 \sin 2\theta + A_3 \sin 3\theta)[1 - \cos(\theta + \beta)] \sin \theta \, d\theta$$

which finally leads to

$$\begin{aligned}
 S_0 b^{-2} \equiv J_0 = 2(1 - \cos \beta) + \sin \beta(\beta - \sin 2\beta) \\
 + A_1(\beta + \frac{4}{3} \sin \beta - \frac{3}{2} \sin 2\beta + \frac{1}{6} \sin 4\beta) \\
 + A_2(\frac{1}{2}\beta \cos \beta - \frac{1}{2} \sin \beta + \frac{1}{6} \sin^3 \beta - 2 \sin^5 \beta) \\
 + \frac{2}{15} A_3 \sin \beta[\cos \beta(2 + \sin^2 \beta + 24 \sin^4 \beta) - 2]. \tag{3.20}
 \end{aligned}$$

The factor  $b^2$  can be eliminated by using Eq. (3.18) to give

$$\mu \equiv S_0/S = J_0/J. \tag{3.21}$$

Again, for a symmetric profile normal to the free stream,  $\beta = \pi/2$ , and  $A_2 = 0$ , it can be verified from Eqs. (3.18) and (3.20) that  $\mu = \frac{1}{2}$ . For small values of  $\beta$  (corresponding to small  $\alpha$ , as can be seen from Eq. (3.5b), Eq. (3.21) reduces to

$$\mu = \frac{1}{4}\frac{7}{8}\beta^4 + 0(\beta^5) \quad (3.22)$$

which shows that the stagnation point is extremely close to the leading edge for small angles of attack.

Knowing the position of the stagnation point, the moment  $M_0$  about the leading edge then becomes, for profiles of small camber,

$$M_0 = M + (Y \cos \alpha + X \sin \alpha)S_0 \quad (3.23)$$

Having obtained  $M_0$ , we can determine the location of the center of pressure, measured from the leading edge, to be approximately at

$$S_1 = M_0/(Y \cos \alpha + X \sin \alpha), \quad (3.24)$$

or, in percentage of the chord,

$$\nu = S_1/S = \mu + (M/S)(Y \cos \alpha + X \sin \alpha)^{-1}. \quad (3.25)$$

Now, consider again a symmetric profile normal to the free stream,  $\alpha = \beta = \pi/2$ . We have shown before that  $\mu = \frac{1}{2}$  and  $M = 0$ , hence  $\nu = \frac{1}{2}$ . For small values of  $\alpha$  ( $\beta$  is also small as previously explained), Eq. (3.22) states that  $\mu$  is very small; Eq. (3.16) reduces to  $Y \cong \pi\rho b^2(\beta + A_1 + A_2/2)$ ; Eq. (3.18) gives  $S \cong 4b^2$ ; and  $M \cong 2\pi b^4\rho[\frac{5}{8}(\beta + A_1 + A_2/2) + \frac{1}{4}(A_1 + 2A_2)]$  from Eq. (3.19). Thus, for small  $\alpha$  and  $\sigma$ , we have approximately

$$\nu \cong \frac{5}{16} + \frac{1}{8}(A_1 + 2A_2)/(\beta + A_1 + A_2/2) + 0(\beta). \quad (3.26)$$

Hence the center of pressure ranges from  $\frac{5}{16}$  to  $\frac{1}{2}$  of the chord.

c. *Some Basic Features of the Free Streamlines.* In this section the shape of the free streamlines  $AD$ ,  $BD'$  and the location of the points  $D$  and  $D'$  will now be calculated. First, we show that the assumed curvature form of the free streamlines, namely, concave towards the cavity, imposes certain conditions on the coefficients  $A_1$ ,  $A_2$  and  $A_3$ . Denote the distance along the streamline  $\psi = 0$  by  $s$ , positive when away from the point  $C$ . On  $AD$ ,  $\zeta = -\xi$  with  $1 \geq \xi \geq \xi_1$  where  $-\xi_1$  is the value of  $\zeta$  at  $D$ ; while on  $BD'$ ,  $\zeta = \xi$  with  $1 \geq \xi \geq \xi_2$  where  $\xi_2 = \zeta_{D'}$ . Then the radius of curvature  $R = -ds/d\theta$  on  $AD$  and  $R = ds/d\theta$  on  $BD'$  should both be positive. We shall first consider  $R$  on  $AD$ . From the definition of  $\Omega = \Theta + iT$  and  $z(\zeta)$  (see Eqs. (3.2), (3.6)),  $\omega$  and  $\Omega$  are both real on  $AD$ , and hence

$$\begin{aligned} R &= -\frac{ds}{d\theta} = -\frac{|dz|}{d\xi} \frac{d\xi}{d\Theta} \frac{d\Theta}{d\theta} = -\frac{\theta}{\Theta} \frac{|dz|}{d\xi} \bigg/ \frac{d\Theta}{d\xi} \\ &= \frac{b^2}{2} \left( -\frac{\theta}{\Theta} \right) \xi^{-3} \frac{(1 - \xi^2)(1 - 2\xi \cos \beta + \xi^2)^2}{2 \sin \beta + (1 - 2\xi \cos \beta + \xi^2)(A_1 - 2A_2\xi + 3A_3\xi^2)}. \end{aligned}$$

From this equation it follows that the condition  $R(\xi) \geq 0$  for  $\xi \leq 1$  requires

$$2 \sin \beta + (1 - 2\xi \cos \beta + \xi^2)(A_1 - 2A_2\xi + 3A_3\xi^2) > 0. \quad (3.27)$$

Consequently  $R(\xi)$  increases from  $R(1) = 0$  as  $\xi$  decreases from 1. A similar requirement for positive  $R$  on  $BD'$  is, for  $\xi_2 \leq \xi \leq 1$ ,

$$2 \sin \beta + (1 + 2\xi \cos \beta + \xi^2)(A_1 + 2A_2\xi + 3A_3\xi^2) > 0. \quad (3.28)$$

It will be only stated here that these two subsidiary conditions are in general satisfied owing to the facts that the coefficient of the first term in Eq. (3.4) is positive and that  $A_n$ 's decrease rapidly with respect to  $A_1$ . However, no further elaboration will be made here on these points.

A parametric representation  $x(\xi), y(\xi)$  of the free streamline  $AD$  can be obtained by integrating Eq. (3.6) along  $\zeta = -\xi$  from  $\xi = 1$  to  $\xi \geq \xi_1$ . On  $AD$ ,  $\tau = \text{Im } \omega = 0$ , and hence, referring to the point  $A$ , we have

$$x - x_A = -\frac{S}{2J} \int_1^\xi \xi^{-3}(1 - 2\xi \cos \beta + \xi^2)(1 - \xi^2) \cos \theta \, d\xi, \quad (3.29)$$

$$y - y_A = -\frac{S}{2J} \int_1^\xi \xi^{-3}(1 - 2\xi \cos \beta + \xi^2)(1 - \xi^2) \sin \theta \, d\xi. \quad (3.30)$$

In the above equations  $\cos \theta$  and  $\sin \theta$  are complicated functions of  $\xi$ ,

$$\theta = -(\Theta^2 - \varepsilon^2)^{\frac{1}{2}}, \quad (3.31)$$

$$\Theta = -2 \tan^{-1} \frac{\xi \sin \beta}{1 - \xi \cos \beta} - A_1\xi + A_2\xi^2 - A_3\xi^3. \quad (3.32)$$

To simplify the calculation, we approximate Eq. (3.31) by  $\theta = -(\Theta + \varepsilon)$  on  $AD$ , which should be good for  $\theta$  both small and large. Then we obtain the following approximate formulas

$$\cos \theta = (1 - 2\xi \cos \beta + \xi^2 \cos 2\beta)/(1 - 2\xi \cos \beta + \xi^2),$$

$$\sin \theta = \frac{2\xi(1 - \xi \cos \beta) \sin \beta + (A_1\xi - A_2\xi^2 - \varepsilon)(1 - 2\xi \cos \beta + \xi^2 \cos 2\beta)}{1 - 2\xi \cos \beta + \xi^2}.$$

Substituting these values into Eqs. (3.29), (3.30) and carrying out the integrations, we finally obtain

$$2J(x - x_A)/S \cong \frac{1}{2}(1 - \xi^2)(\xi^{-2} - \cos 2\beta) - 2 \cos \beta(1 - \xi)^2\xi^{-1} + 2 \sin^2 \beta \log \xi; \quad (3.33)$$

$$2J(y - y_A)/S \cong (2 \sin \beta + A_1 + 2\varepsilon \cos \beta)(1 - \xi)^2/\xi - \varepsilon \left( \frac{1 - \xi^2}{2\xi^2} + \log \xi \right) + (\sin 2\beta + 2A_1 \cos \beta + A_2 + \varepsilon \cos 2\beta) [\log \xi + \frac{1}{2}(1 - \xi^2)] \quad (3.34)$$

$$+ \frac{1}{3}(A_1 \cos 2\beta + 2A_2 \cos \beta)(1 - \xi)^2(2 + \xi) - \frac{1}{4}A_2(1 - \xi^2)^2 \cos 2\beta$$

To find the location of  $D$ ,  $(x_D, y_D)$ , we first determine the value  $\xi_1$  corresponding to  $\Omega = -\varepsilon$ . Then, by letting  $\Omega = -\varepsilon$  and  $\zeta = -\xi_1$  in Eq. (3.4), we obtain

$$\xi_1 = \frac{\varepsilon}{a_1} \left[ 1 + \frac{a_2 \varepsilon}{a_1^2} + 0(\varepsilon^2) \right].$$

Using this value of  $\xi_1$ , one can easily derive from Eqs. (3.33), (3.34) that

$$x_D \cong \frac{S}{J} \left\{ \frac{a_1^2}{4\varepsilon^2} + 0\left(\frac{1}{\varepsilon}\right) \right\} = \frac{S}{J} \left( \frac{2 \sin \beta + A_1}{\sigma} \right)^2 [1 + 0(\sigma)], \quad (3.35)$$

$$y_D \cong \frac{S}{J} \left\{ \frac{a_1^2}{2\varepsilon} + 0(\log \varepsilon) \right\} = \frac{S}{J} \frac{(2 \sin \beta + A_1)^2}{\sigma} [1 + 0(\sigma \log \sigma)]. \quad (3.36)$$

The above value of  $x_D$  and  $y_D$  may be regarded respectively as the half-length and half-width of the cavity. Thus we see that for  $\sigma$  small the cavity length is proportional to  $\sigma^{-2}$ , while the cavity width, proportional to  $\sigma^{-1}$ . It may also be seen that the free streamline near  $D$  lies close to a parabola

$$y^2/x \cong a_1^2 S/J = b^2(2 \sin \beta + A_1)^2 \equiv C, \quad \text{say.}$$

Then a comparison with Eq. (3.15) shows that the drag  $X$  can be expressed by

$$X \cong \pi \rho b^2 (\sin \beta + A_1/2)^2 = \pi \rho C/4$$

which is the general formula of Levi-Civita (16).

Now, in order to determine these unknown coefficients  $A_1, A_2, A_3$  and  $\beta$  and thus to exhibit explicitly the effects of cavitation number  $\sigma$ , the attack angle  $\alpha$  and the profile geometry, two specific examples, the circular arc and the flat plate, will be worked out below.

**IV. Cavitating Hydrofoils with Circular Arc and Flat Plate Profile.** Let us first consider the hydrofoil having the circular arc profile, with radius  $R$  and arc angle  $2\gamma$  (see Fig. 3). The flat plate is just a special case with  $\gamma \rightarrow 0$  ( $R \rightarrow \infty$ ).

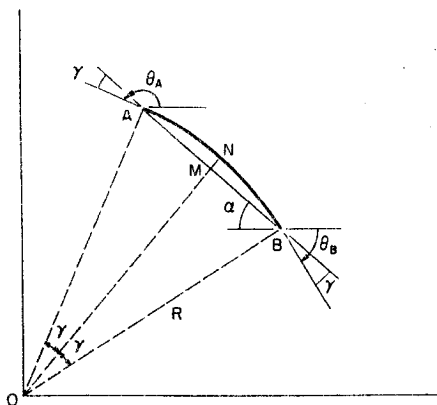


FIG. 3. The circular arc profile

We shall here restrict ourselves to small values of  $\gamma$ , say,  $\gamma < \pi/4$ . The arc length  $S$  and the length  $l$  of the chord  $AB$  are then

$$S = 2\gamma R; \quad l = 2R \sin \gamma = 2\gamma R(1 - \gamma^2/6). \tag{4.1}$$

Now we choose the end points  $A$  and  $B$  to which the following boundary conditions are applied:

$$\begin{aligned} \text{(i) } \theta_A &= \pi - \alpha + \gamma, & \text{(ii) } \theta_B &= -\alpha - \gamma, \\ \text{(iii), (iv) radius of curvature at } A \text{ and } B &= R = S/2\gamma. \end{aligned} \tag{4.2}$$

These four conditions enable us to determine  $A_1, A_2, A_3$  and  $\beta$  which in turn can be used to check the radius of curvature at other points on the boundary. Applying (i) and (ii) to the definition of  $\theta$  (see Eqs. (3.2), (3.5)), we obtain

$$\theta_B = (\theta_B^2 + \varepsilon^2)^{\frac{1}{2}} = [(\alpha + \gamma)^2 + \varepsilon^2]^{\frac{1}{2}} = \beta + A_1 + A_2 + A_3,$$

$$\theta_A = -(\theta_A^2 + \varepsilon^2)^{\frac{1}{2}} = -\pi + \alpha - \gamma - \frac{1}{2}\varepsilon^2/\theta_A = -\pi + \beta - A_1 + A_2 - A_3.$$

In the second equation the value with  $\frac{1}{2}$  power is expanded for  $\theta_A$  is always much greater than  $\varepsilon$ , but in the first equation no expansion is made because the ratio  $\varepsilon/\theta_B$  may not be small. Adding and subtracting these two equations, we have

$$A_1 + A_3 = \gamma + \frac{1}{2} \{[(\alpha + \gamma)^2 + \varepsilon^2]^{\frac{1}{2}} - (\alpha + \gamma)\} + \frac{\varepsilon^2}{4} (\pi - \alpha + \gamma)^{-1} \tag{4.3}$$

$$\beta + A_2 = \alpha + \frac{1}{2} \{[(\alpha + \gamma)^2 + \varepsilon^2]^{\frac{1}{2}} - (\alpha + \gamma)\} - \frac{\varepsilon^2}{4} (\pi - \alpha + \gamma)^{-1}. \tag{4.4}$$

In applying the conditions (iii), (iv), we first note that at  $B, \tau = 0$  and

$$\frac{d\theta}{d\eta} = \frac{(\theta_B^2 + \varepsilon^2)^{\frac{1}{2}}}{\theta_B} \frac{d\theta}{d\eta} \rightarrow - \frac{(\theta_B^2 + \varepsilon^2)^{\frac{1}{2}}}{\theta_B} (A_1 + 4A_2 + 9A_3) \sin \eta, \quad \text{as } \eta \rightarrow 0.$$

Hence, from Eq. (3.10)

$$- \frac{\theta_B(1 + \cos \beta)}{(\theta_B^2 + \varepsilon^2)^{\frac{1}{2}}} (A_1 + 4A_2 + 9A_3)^{-1} = \frac{R}{2b^2} = \frac{RJ}{2S} = \frac{J}{4\gamma};$$

or,

$$A_1 + 4A_2 + 9A_3 = (4\gamma/J)(\alpha + \gamma)[(\alpha + \gamma)^2 + \varepsilon^2]^{-\frac{1}{2}}(1 + \cos \beta). \tag{4.5}$$

Similarly, application of the boundary condition (iv) at  $A$  yields

$$A_1 - 4A_2 + 9A_3 = (4\gamma/J)(1 - \cos \beta)[1 + 0(\varepsilon^2)]. \tag{4.6}$$

In Eqs. (4.5) and (4.6),  $J$ , as defined by Eq. (3.18), also contains  $A_1, A_2, A_3$  and  $\beta$ . Thus Eqs. (4.3)-(4.6) together with (3.18) represent five transcendental equations for five unknowns  $A_1, A_2, A_3, \beta$  and  $J$ . The solution, however, can easily be approximated with good accuracy by using an iteration procedure. For the present purpose, the following approximation is sufficient



$$\beta = \alpha + \frac{1}{2}\delta - \frac{\varepsilon^2}{4(\pi - \alpha + \gamma)} - \frac{\gamma}{4 + \pi \sin \alpha} \left\{ \frac{\alpha + \gamma}{[(\alpha + \gamma)^2 + \varepsilon^2]^{\frac{1}{2}}} \cos^2 \frac{\alpha}{2} - \sin^2 \frac{\alpha}{2} \right\} \quad (4.7a)$$

$$\delta = [(\alpha + \gamma)^2 + \varepsilon^2]^{\frac{1}{2}} - (\alpha + \gamma); \quad (4.7b)$$

$$A_1 = \gamma \left\{ 1 + \frac{\pi \sin \alpha}{8(4 + \pi \sin \alpha)} \right\} + \frac{9}{16} \delta \left\{ 1 + \frac{\gamma(1 + \cos \alpha)}{9[(\alpha + \gamma)^2 + \varepsilon^2]^{\frac{1}{2}}} \right\} + \frac{9\varepsilon^2}{32(\pi - \alpha + \gamma)}; \quad (4.8)$$

$$A_2 = \frac{\gamma}{4 + \pi(A_1 + \sin \beta)} \left\{ \frac{\alpha + \gamma}{[(\alpha + \gamma)^2 + \varepsilon^2]^{\frac{1}{2}}} \cos^2 \frac{\beta}{2} - \sin^2 \frac{\beta}{2} \right\}; \quad (4.9)$$

$$A_3 = \frac{1}{9}(\gamma - A_1) - \frac{\gamma}{9(4 + \pi \sin \alpha)} \left\{ \pi \sin \beta + \frac{2\delta(1 + \cos \alpha)}{[(\alpha + \gamma)^2 + \varepsilon^2]^{\frac{1}{2}}} \right\}; \quad (4.10)$$

whereas  $J$  is still given by (3.18). The above result shows that  $(\beta - \alpha)$ ,  $A_1$ ,  $A_2$  and  $A_3$  are all of  $O(\gamma, \varepsilon^2)$  for all  $\alpha$ ; and in particular,  $(\beta - \alpha)$ ,  $A_2$  and  $A_3$  reduce to  $O(\gamma\varepsilon^2, \varepsilon^4)$  for  $\alpha$  close to  $\pi/2$ . Moreover, the fact that  $A_3$  is much smaller than  $A_1$  indicates a good accuracy of the expansion given by Eq. (3.13). If the above quantities are used to check the curvature and slope of the solid boundary at some other points, say at  $\zeta = e^{i\pi/2}$ , one can easily find that the agreement is within a factor at most of  $O(\gamma, \varepsilon^2)$ . It should also be remarked here that if more terms were taken in the expansion (3.13), then the first three coefficients  $A_1$ ,  $A_2$ ,  $A_3$  would differ slightly from the above value (4.8-4.10). However, it can be verified that the "improvement" of the solution by taking terms more than three is actually unappreciable.

Now we define the conventional drag coefficient, lift coefficient and moment coefficient (about the leading edge) as follows:

$$X = \frac{1}{2}\rho U^2 l C_D; \quad Y = \frac{1}{2}\rho U^2 l C_L; \quad M_0 = \frac{1}{2}\rho U^2 l^2 C_{M_0}. \quad (4.11)$$

Then, for  $\gamma$  not too large ( $< \pi/4$ ), we compile some of the previous results and note that  $U = (1 + \sigma)^{-\frac{1}{2}}$ , we finally obtain:

$$C_D = \frac{2\pi}{J} \left( 1 + \sigma + \frac{\varepsilon^2}{6} + \frac{\gamma^2}{6} \right) \left[ \sin \beta + \frac{A_1}{2} \right]^2; \quad (4.12)$$

$$C_L = \frac{2\pi}{J} \left( 1 + \sigma + \frac{\varepsilon^2}{4} + \frac{\gamma^2}{6} \right) \left\{ \left[ \sin \beta \cos \beta + A_1 \cos \beta + \frac{A_2}{2} \right] + \frac{\varepsilon^2}{4} \frac{\cos \beta}{(\sin \beta + A_1/2)^4} \left[ \left( \sin \beta + \frac{A_1}{2} \right)^3 + \sin \beta \left( \sin \beta + \frac{A_1}{4} \right) \left( \frac{A_1}{2} + \frac{5}{4} A_2 + A_3 \right) \right] \right\}; \quad (4.13)$$

$$C_{M_0} = \frac{4\pi}{J^2} \left( 1 + \sigma + \frac{\gamma^2}{3} \right) K + \mu(C_L \cos \alpha + C_D \sin \alpha) \quad (4.14)$$

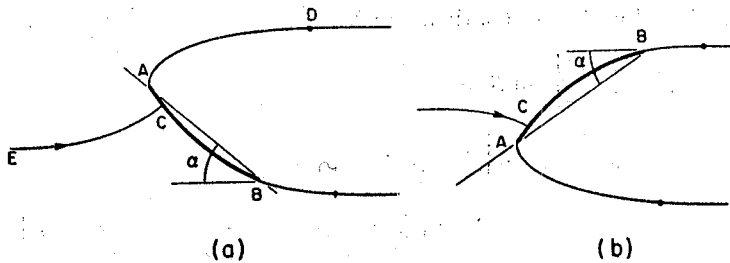


FIG. 4

where  $\beta, A_1, A_2, A_3$  are given by Eqs. (4.7)–(4.10);  $J$  is given by (3.18);  $K$ , by (3.19);  $\mu$ , by (3.20), (3.21) and  $\varepsilon = \frac{1}{2} \log(1 + \sigma)$ .

The results for the flat plate hydrofoil can be deduced from the above expressions by putting  $\gamma = 0$ . For the circular arc hydrofoil with its convex side toward the approaching stream at positive  $\alpha$  (see Fig. 4a), the above formulas still hold if  $\gamma$  assumes a negative value. For flow configurations with positive  $\gamma$  but negative  $\alpha$  (see Fig. 4b), the results are that  $C_D$  stays the same, but  $C_L$  and  $C_M$  have opposite signs as those of flow case (4a).

There are however, several points of complication at which the above results may become invalid, and thus should be applied with great care. First, there in general exists a certain small  $\alpha$ , say,  $\alpha_p$ , positive or negative, at which the free streamline  $AD$  given by Eqs. (3.33), (3.34) would cut into the solid boundary. It could be conjectured that a partial cavitation, that is, with the rear end of the cavity reattached to the boundary, probably is established for  $\alpha$  around  $\alpha_p$ . The present theory certainly does not cover partially cavitating flows. Second there is another critical value of  $\alpha$ , say,  $\alpha_c(\gamma, \sigma)$  at which  $\beta = 0$ , implying that the stagnation point is then at the leading edge. Hence the cavity will shift side on the boundary for  $\alpha < \alpha_c$ . The value of  $\alpha_c$  is in general less than  $\alpha_p$ . Third, in flow configurations shown in Fig. 4, the streamline will be in a more critical position at  $B$  than at  $A$ . In other words, the flow is more likely to separate in front of  $B$  for small enough  $\alpha$ ; and thus a rear part of the boundary will be inside the full cavity. This critical condition will take place when either the slope or the radius of curvature of streamline  $BD'$  at  $B$  is numerically greater than that of the solid boundary at  $B$ . These points will be touched upon in the following explicit calculations, though the clarification of these points requires further study.

a. *Inclined Flat Plate.* For an inclined flat plate,  $\gamma = 0$ , and hence Eqs. (4.7)–(4.10) reduce to

$$\beta = \alpha + \frac{1}{2}[(\alpha^2 + \varepsilon^2)^{\frac{1}{2}} - \alpha] - \frac{1}{4}\varepsilon^2/(\pi - \alpha), \tag{4.15}$$

$$A_1 = \frac{9}{16}[(\alpha^2 + \varepsilon^2)^{\frac{1}{2}} - \alpha] + \frac{9}{32}\varepsilon^2/(\pi - \alpha), \quad A_2 = 0, \quad A_3 = -\frac{1}{3}A_1 \tag{4.16}$$

and

$$J = 4 + \pi \sin \beta + A_1(\pi + 2.72 \sin \beta). \tag{4.17}$$

The expressions for  $C_L$  and  $C_D$  then can be simplified to:

$$C_D \cong \frac{2\pi}{J} \left( 1 + \sigma + \frac{\varepsilon^2}{6} \right) \left[ \sin \beta + \frac{A_1}{2} \right]^2, \quad (4.18)$$

$$C_L \cong \frac{2\pi}{J} \left( 1 + \sigma + \frac{\varepsilon^2}{4} \right) \cos \beta \left[ (\sin \beta + A_1) + \frac{\varepsilon^2}{32} \frac{8 \sin \beta (\sin \beta + A_1)^2 + A_1^2 (A_1 - \sin \beta)}{(\sin \beta + A_1/2)^4} \right]. \quad (4.19)$$

In the idealized case of  $\sigma = 0$  (hence  $\varepsilon = 0$ ),  $\beta = \alpha$  and  $A_1, A_2, A_3$  all vanish, the above result then reduces to Rayleigh's theory of the oblique lamina (e.g. ref. 15, p. 102):

$$C_D = \frac{2\pi \sin^2 \alpha}{4 + \pi \sin \alpha}; \quad C_L = C_D \cot \alpha. \quad (4.20)$$

When  $\alpha = \pi/2$  but  $\sigma > 0$ , Eqs. (4.17)–(4.19) become

$$C_D \cong \frac{2\pi}{4 + \pi} \left( 1 + \sigma + \frac{1}{6(4 + \pi)} \sigma^2 \right), \quad C_L = 0. \quad (4.21)$$

which agree, up to the term in  $\sigma$ , with the known results (see also Eq. (2.2)).

For general values of  $\alpha$  and  $\sigma$ , one more physical requirement, however, should be pointed out. For a fully cavitating flow past the oblique flat plate, the local pressure is everywhere normal to the plate and, besides, there is no singular force at leading edge as in the noncavitating case. Consequently  $C_L$  and  $C_D$  should satisfy the condition

$$C_D/C_L = \tan \alpha \quad \text{for all } \alpha \text{ and } \sigma. \quad (4.22)$$

In the special cases (i)  $\sigma = 0$ , (ii)  $\alpha$  close to  $\pi/2$  and  $\sigma > 0$ , the above condition is obviously satisfied (see Eqs. (4.20), (4.21)). However, in the general case, it is rather difficult to derive this relation from Eqs. (4.18), (4.19), because of the complicated manner in which the dependence on  $\alpha$  and  $\sigma$  appears. Under this circumstance, the condition (4.22) can only be used as a check in numerical computation to assure the correctness of this theory.

Another approximate formula for  $C_L$ , when  $\alpha$  is small but  $\sigma$  is left arbitrary, has been given by Betz. The main idea is first to linearize the Rayleigh's formula (4.20) to obtain  $\pi\alpha/2$  and then by adding to this quantity the pressure coefficient on the upper suction side, namely,  $\sigma$ , to obtain

$$C_L = \frac{1}{2}\pi\alpha + \sigma. \quad (4.23)$$

This approximation appears, in general, too rough.

On the other hand, as  $\sigma$  increases the cavity dimension diminishes (see Eqs. (3.37), (3.38)); in some cases it is observed experimentally that the cavity collapses completely for  $\sigma$  approximately greater than 1.5. In the latter flow condition  $C_L$  and  $C_D$  then resume their noncavitating (aerodynamic) values:

$$C_L \cong 2\pi \sin \alpha, \quad C_D \cong (2 \cos \alpha) C_f \quad (4.24)$$

where  $C_f$  is the mean friction coefficient on one side of the plate.

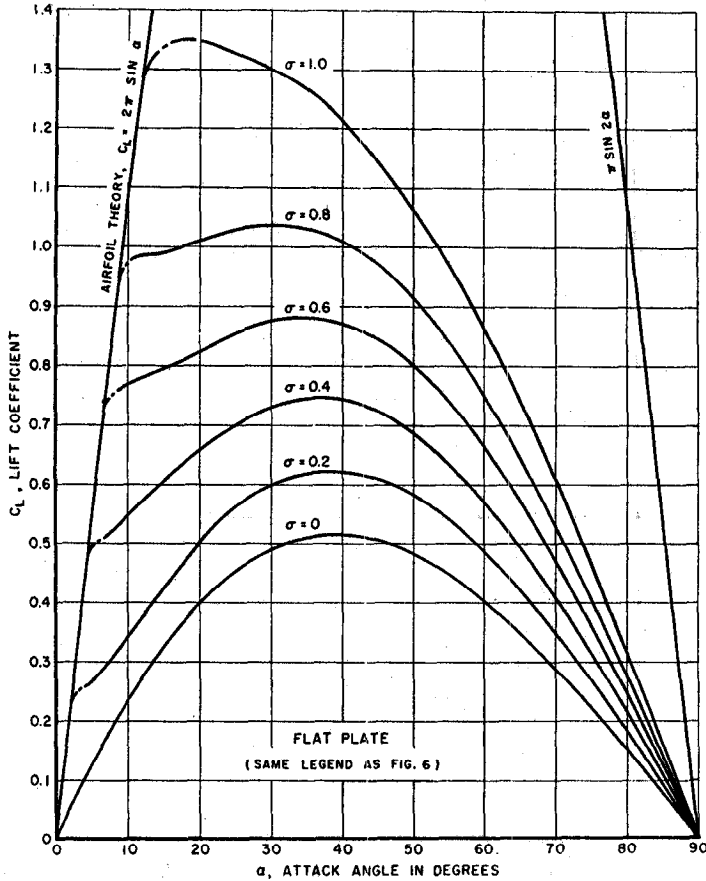


FIG. 5. The dependence of  $C_L$  on  $\alpha$

The value of  $C_L$  given by (4.19) is plotted against  $\alpha$  for different values of  $\sigma$  in Figs. 5 and 6. The aerodynamic value of  $C_L$  given by (4.24) is also shown for comparison. For a given value of  $\sigma$ , there is a certain small  $\alpha$ , say,  $\alpha_p$  at which the cavitating value of  $C_L$  becomes equal to the aerodynamic value if the fully cavitating model is assumed still possible (e.g.  $\alpha_p = 4.5^\circ$  for  $\sigma = 0.4$ ). A further extrapolation (dotted lines) of Eq. (4.19), without justification, to smaller  $\alpha$  would yield an implausible result that the cavitating value of  $C_L$  would be greater than its corresponding aerodynamic value. As a physical conjecture, this result is unacceptable. Instead, we expect that near  $\alpha = \alpha_p$  partially cavitating flow takes place, a transitional stage between the fully cavitating and fully wetted conditions. This argument is supported by experimental evidence, as shown by the double-dotted lines in Figs. 5 and 6. Thus, the aerodynamic value of  $C_L$  for a fully wetted hydrofoil is actually the asymptote to which the cavitating  $C_L$  at every  $\sigma$  approaches from below as  $\alpha$  decreases from  $\alpha_p$ .

The value of  $C_D$  given by Eq. (4.18) is similarly plotted in Figs. 7 and 8. In the cavitating range of practical interest, the Reynolds number of the flow is in general very large, say, of the order  $5 \times 10^5$  or greater. Then the frictional drag

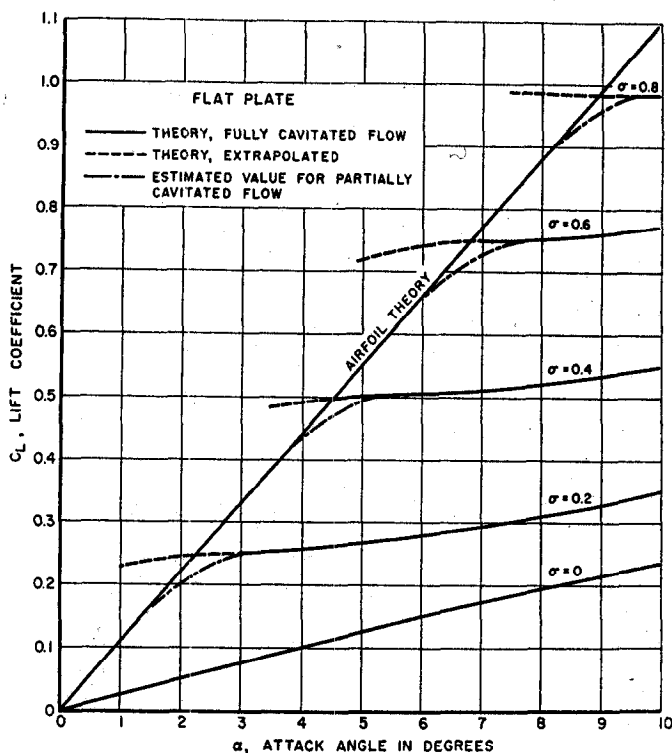


FIG. 6. Values of  $C_L$  for small  $\alpha$

coefficient  $C_f$ , as can be estimated by using the Prandtl-Schlichting formula (e.g. ref. 17, p. 33), is of the order 0.005 which is much smaller than the cavity  $C_D$  for almost all  $\alpha$  and  $\sigma$  and can thus be neglected.

A series of experiments (18) was carried out in the Hydrodynamics Laboratory, California Institute of Technology, at about the same time the present theoretical result was obtained. In order to compare the theory with the experiments,  $C_L$  and  $C_D$  are further cross-plotted against  $\sigma$  in Figs. 9 and 10 in which the experimental data are also shown.\* The agreement is very good. As a further check, the value  $C_L/C_D$  is plotted against  $\alpha$  for several  $\sigma$  and is compared with  $\cot \alpha$  in Fig. 11. The deviation is less than a few percent, implying the accuracy of the present theory.

Some of the salient points of the previous results may be summarized here.

(i) The results plotted in Figs. 9 and 10 show that for  $\alpha$  large, say, greater than  $45^\circ$ , the values of  $C_L$  and  $C_D$  approach respectively the asymptotes

$$C_L(\sigma, \alpha) = (1 + \sigma)C_L(0, \alpha), \quad C_D(\sigma, \alpha) = (1 + \sigma)C_D(0, \alpha), \quad (4.25)$$

\* In these experimental data, the correction due to tunnel-wall effect was not taken into account. However, the cavitation number  $\sigma$  was computed based on the measured cavity pressure which presumably absorbs a part of the wall-effect correction. For the detailed description, refer to Ref. (18).

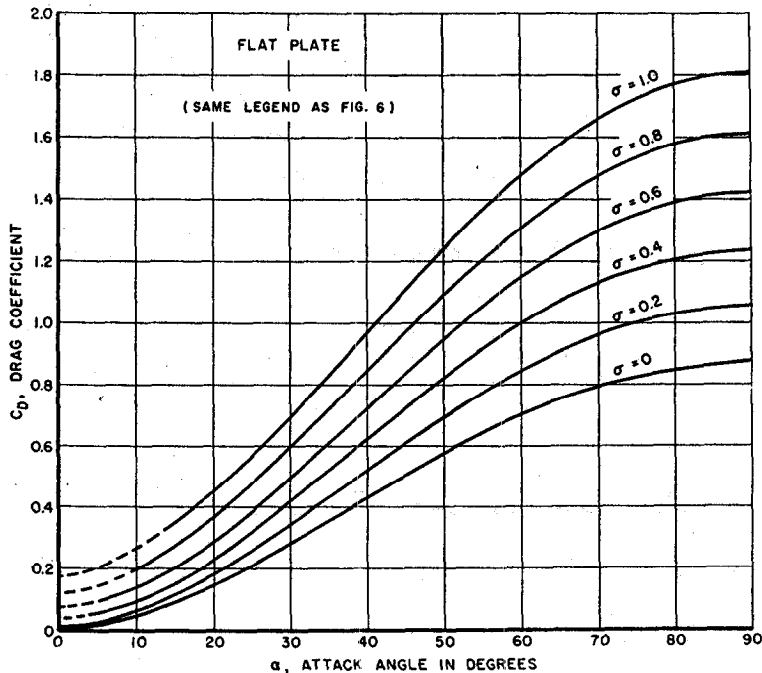


Fig. 7. The dependence of  $C_D$  on  $\alpha$

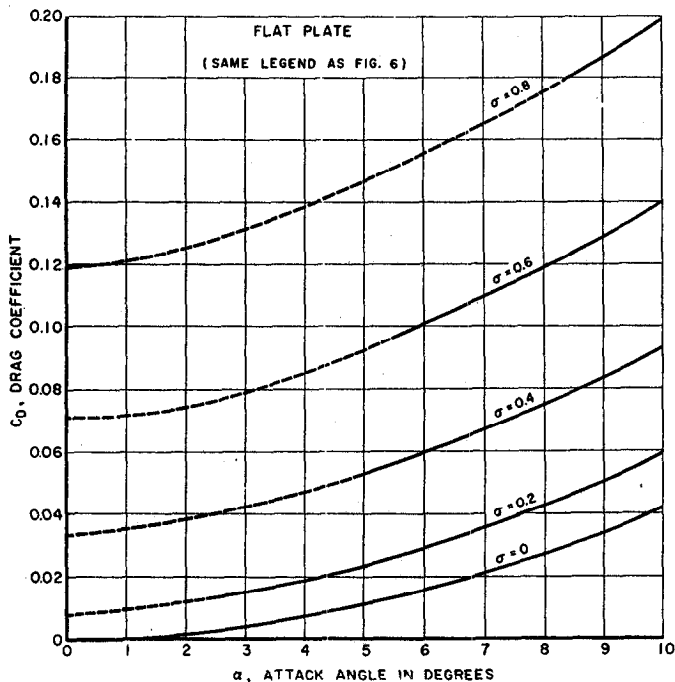


Fig. 8. Values of  $C_D$  for small  $\alpha$

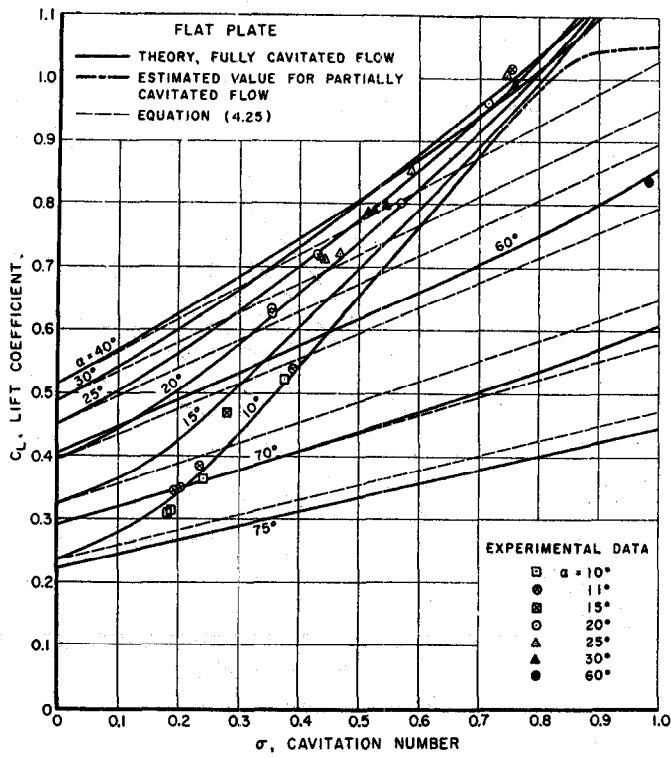


FIG. 9. The dependence of  $C_L$  on  $\sigma$

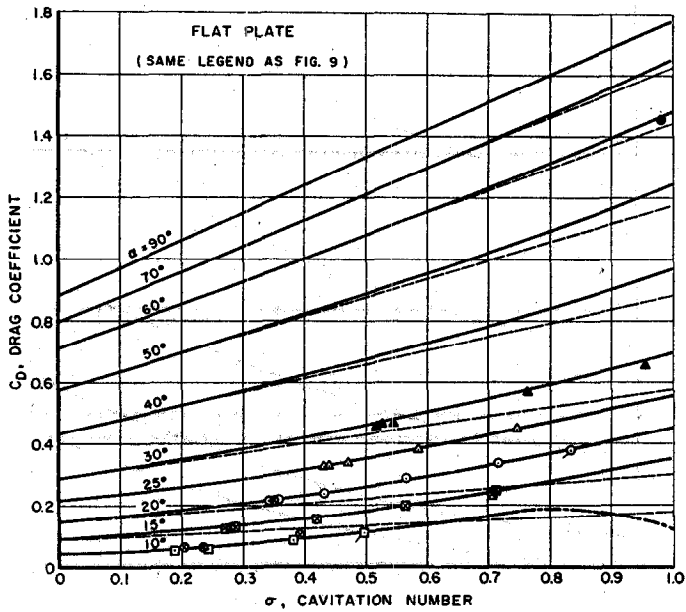


FIG. 10. The dependence of  $C_D$  on  $\sigma$

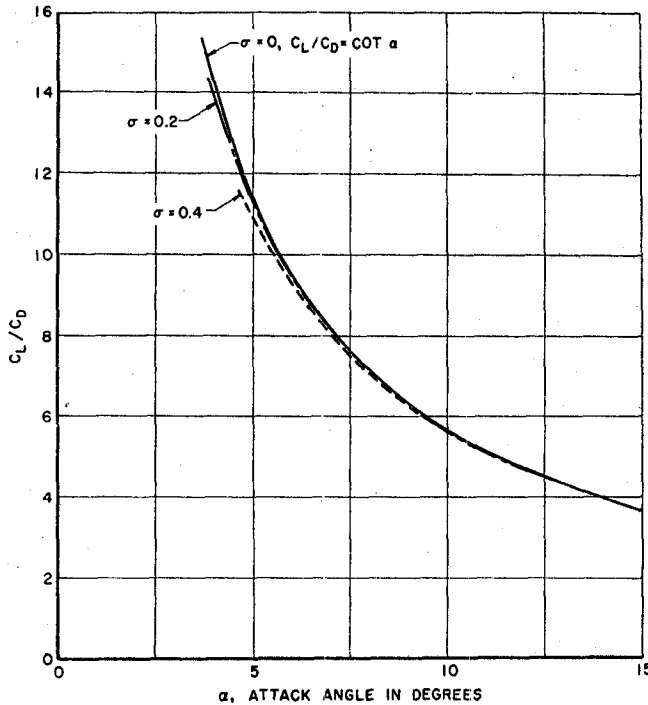


FIG. 11. Values of  $C_L/C_D$  for the flat plate

which are shown as dotted lines. For  $\alpha$  small, they deviate appreciably from these asymptotes; the deviation is much more marked for  $C_L$  since here the deviation of  $C_D$  is magnified by a factor  $\cot \alpha$ . For instance, the slope  $dC_L/d\sigma$  becomes greater than unity for  $\alpha < 15^\circ$  and  $\sigma > 0.2$ .

(ii) It is to be noted from Figs. 5 and 6 that, after the hydrofoil at small  $\alpha$  is fully cavitating,  $dC_L/d\alpha$  decreases to values much smaller than that of fully wetted case, which is approximately equal to  $2\pi$ . This means that fully cavitating hydrofoils are quite insensitive to variations of attack angle  $\alpha$ . However, the drag coefficient is relatively more sensitive due to the relation (4.22). Differentiating Eq. (4.22) with respect to  $\alpha$ , we have

$$\frac{1}{C_D} \frac{dC_D}{d\alpha} = \frac{1}{C_L} \frac{dC_L}{d\alpha} + 2 \csc 2\alpha \tag{4.26}$$

Thus, the percentagewise change of  $C_D$  is always greater than that of  $C_L$ .

The location of the stagnation point,  $\mu = S_0/S$ , as given by Eqs. (3.18) and (3.20), is plotted in Fig. 12 for this oblique flat plate by using the quantities given in Eqs. (4.15)–(4.17). It is of interest to note that  $\sigma$  has really negligible effect on  $\mu$ . With the aid of Figs. 9, 10 and 12, the moment coefficient  $C_{M_0}$  about the leading edge of the flat plate (see Eq. (4.14) with  $\gamma = 0$ ) is further computed and plotted against  $\sigma$  in Fig. 13. The theoretical value of  $C_{M_0}$  is also in fair agree-



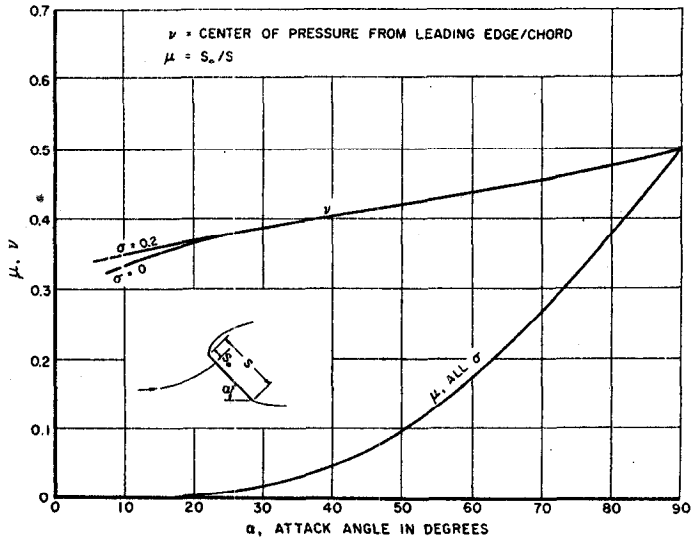


Fig. 12. Location of stagnation point and center of pressure (flat plate)

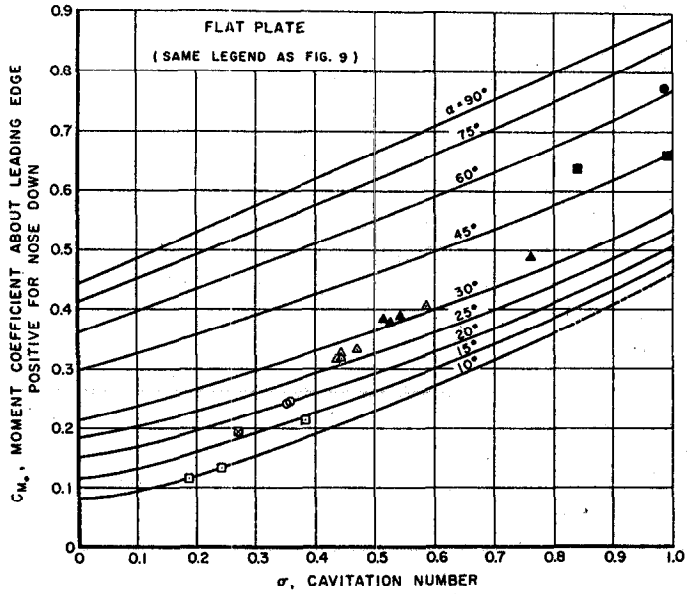


Fig. 13

ment with the experimental data (18). From these results the location of the center of pressure

$$\nu = C_{M_0} / (C_L \cos \alpha + C_D \sin \alpha) \quad (4.27)$$

can be easily deduced. The result shows that  $\nu$ , like  $\mu$ , is also independent of  $\sigma$  for all practical range of  $\sigma$  (see Fig. 12). It varies almost linearly from one-third chord at small  $\alpha$  to half-chord at  $\alpha = \pi/2$ .

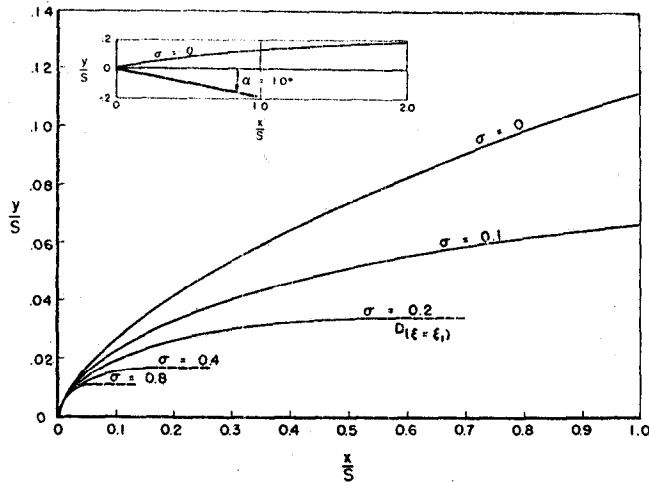


FIG. 14. Some calculated locations of the free streamline

The location of the free streamlines, as given by Eqs. (3.33), (3.34), is computed and plotted for  $\alpha = 10^\circ$  in Fig. 14.

b. *An Example of Circular Arc Hydrofoils; Further Discussions.* With a knowledge of some essential hydrodynamic features of the flat plate hydrofoil, we may further note several general characteristics of the camber effect in cavity flows by examining the circular arc profile.

First, when both  $\gamma$  and  $\epsilon$  are assumed to be small, then at  $\alpha = \pi/2$ , we have

$$A_1 \cong \gamma + \frac{9}{8\pi} \epsilon^2, \quad A_3 \cong -\frac{\epsilon^2}{8\pi} - 0.05\gamma, \quad A_2 \text{ and } (\beta - \alpha) = 0(\gamma\epsilon^2);$$

and hence

$$C_D \cong \frac{2\pi}{4 + \pi} (1 + \sigma) \left[ 1 + \frac{4\gamma}{3(4 + \pi)} \right], \quad C_L = 0. \quad (4.28a)$$

Therefore

$$\left( \frac{dC_D}{d\gamma} \right)_{\alpha=\pi/2} \cong \frac{8\pi}{3(4 + \pi)^2} (1 + \sigma) \cong \frac{1}{6} (1 + \sigma). \quad (4.28b)$$

These equations then represent the effect of camber on pure drag problems.

Second, in order to exhibit the effect of camber on  $C_L$  and  $C_D$  for all  $\alpha$ , we consider the limiting case  $\epsilon \rightarrow 0$  and  $\gamma \rightarrow 0$ , in which case

$$\frac{dA_1}{d\gamma} \rightarrow 1, \quad \frac{dA_2}{d\gamma} = -\frac{d\beta}{d\gamma} \rightarrow \frac{\cos \alpha}{4 + \pi \sin \alpha}.$$

It then follows from Eqs. (4.12), (4.13) that as  $\epsilon \rightarrow 0$ ,  $\gamma \rightarrow 0$ ,

$$\frac{dC_L}{d\gamma} \cong \frac{7\pi \cos \alpha}{(4 + \pi \sin \alpha)^2} \left\{ 1 + \frac{16}{21} \sin \alpha + \frac{4}{7} \sin^2 \alpha \right\}; \quad (4.29)$$

$$\frac{dC_D}{d\gamma} \cong \frac{4\pi \sin \alpha}{(4 + \pi \sin \alpha)^2} \left\{ 1 - \frac{1}{3} \sin^2 \alpha + \frac{\pi \sin \alpha \cos^2 \alpha}{4(4 + \pi \sin \alpha)} \right\}. \quad (4.30)$$

Therefore,

$$\frac{dC_L}{d\gamma} \rightarrow \frac{7\pi}{16}, \quad \frac{dC_D}{d\gamma} \rightarrow 0 \quad \text{as } \alpha \rightarrow 0, \gamma \rightarrow 0 \text{ and } \varepsilon \rightarrow 0, \quad (4.31)$$

$$\frac{dC_D}{d\gamma} \rightarrow \frac{8\pi}{3(4 + \pi)^2}, \quad \frac{dC_L}{d\gamma} \rightarrow 0 \quad \text{as } \alpha \rightarrow \frac{\pi}{2}, \gamma \rightarrow 0 \text{ and } \varepsilon \rightarrow 0. \quad (4.32)$$

This result shows that for small  $\alpha$  positive camber is very favorable for increasing  $C_L$  with negligible effect on  $C_D$ . On the other hand, when  $\sigma$  is so large that the hydrofoil is fully wetted, then we obtain the well-known aerodynamic value of  $C_L$ :

$$C_L = 2\pi \sin \left( \alpha + \frac{\gamma}{2} \right), \quad (4.33)$$

from which we derive

$$\left( \frac{dC_L}{d\gamma} \right)_{\alpha \rightarrow 0, \gamma \rightarrow 0} = \pi. \quad (4.34)$$

Although the value of  $dC_L/d\gamma$  for fully cavitated hydrofoil is less than that in fully wetted flow, a comparison, however, can be made on a different basis. If we compare these values at the same effective angle of attack (aerodynamic)

$$\alpha_e = \alpha + \frac{1}{2}\gamma,$$

then the aerodynamic value of  $C_L$  is almost the same for same  $\alpha_e$ , but the cavitated value of  $C_L$  still increases with increase in  $\gamma$ , holding  $\alpha_e$  fixed. The rate of increase in this case can be estimated to be  $dC_L/d\gamma = \frac{1}{2}$  at equal  $\alpha_e$ . The in-

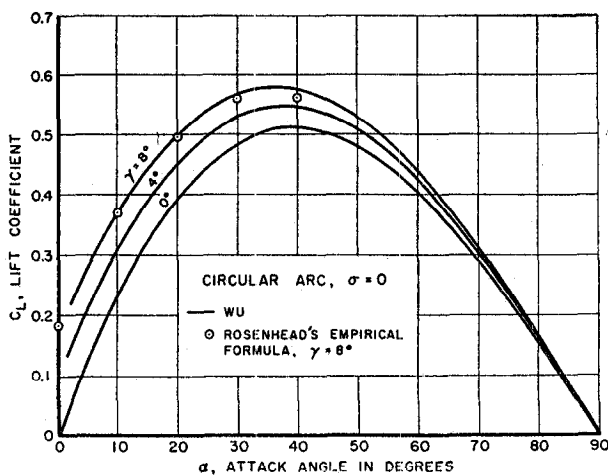


FIG. 15. Effect of camber on  $C_L$  at  $\sigma = 0$

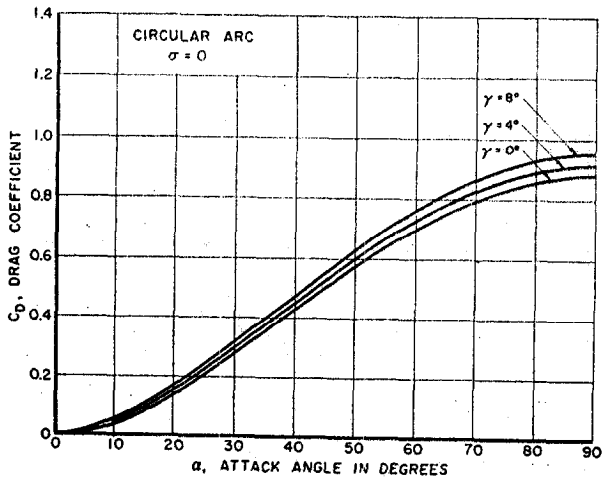


Fig. 16. Effect of camber on  $C_D$  at  $\sigma = 0$

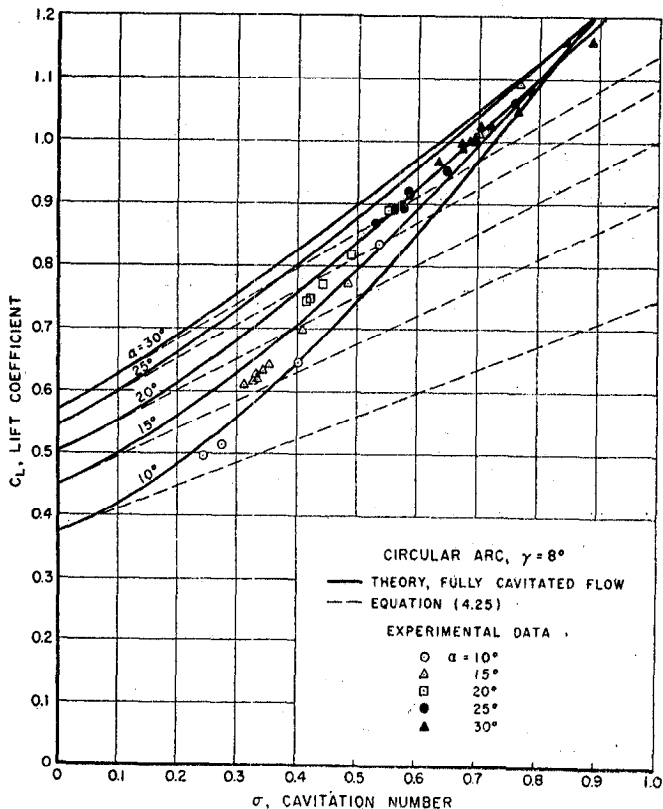
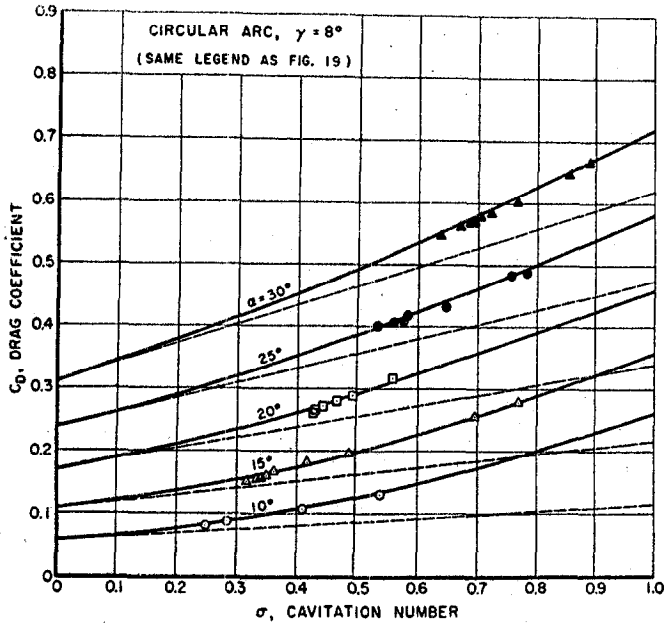


Fig. 17



fluence of  $\gamma$  on  $C_L$  and  $C_D$  at  $\sigma = 0$  is shown in Figs. 15 and 16 for two particular values of  $\gamma$ ,  $4^\circ$  and  $8^\circ$ .

Rosenhead proposed an empirical formula for small cambers at  $\sigma = 0$  as follows (2):

$$C_P = \frac{2\pi \sin \alpha}{4 + \pi \sin \alpha} + \frac{20\pi}{9} \frac{2 + \cos \alpha + 3 \cos^2 \alpha}{(4 + \pi \sin \alpha)^2} \tan \frac{\gamma}{2} \quad (4.35a)$$

and

$$C_L = C_P \cos \delta, \quad C_D = C_P \sin \delta \quad (4.35b)$$

where the angle  $\delta$  can be computed according to Rosenhead's formulation. The value of  $\delta$  is in general very close to  $\alpha$ . Equation (4.35) is plotted in Fig. 15 for several points with  $\gamma = 8^\circ$ . The result shows that this formula is in good agreement with the present theory for  $\alpha$  small.

Finally, we present here some explicit results of a numerical example with  $\gamma = 8^\circ$  to show the over-all effects due to  $\sigma$ ,  $\alpha$  and  $\gamma$ . Since both  $C_L(\sigma, \gamma, \alpha)$  and  $C_D(\sigma, \gamma, \alpha)$  approach their asymptotes  $(1 + \sigma)C_L(0, \gamma, \alpha)$  and  $(1 + \sigma)C_D(0, \gamma, \alpha)$  for  $\alpha$  large, the calculation is limited here to  $\alpha \leq 30^\circ$ . For  $10^\circ < \alpha < 30^\circ$ , the calculated values of  $C_L$  and  $C_D$  are plotted against  $\sigma$  in Figs. 17 and 18 together with some experimental data (18). The agreement here may also be considered as good.

**Acknowledgments.** The author wishes to express his great appreciation for many useful discussions with Professors M. S. Plesset and H. S. Tsien. He also

wishes to thank Dr. B. R. Parkin for his interest in planning an experimental program in order to check the present theory, and for his courtesy in furnishing the data used here. He also thanks Miss Z. Lindberg for her help in numerical computations.

## REFERENCES

1. POOLE, E. G. C., "On the Discontinuous Motion Produced in an Infinite Stream by Two Plate Obstacles," *Proc. London Math. Soc.*, Vol. 22 (2), p. 425, 1924.
2. ROSENHEAD, L., "Resistance to a Barrier in the Shape of an Arc of a Circle," *Proc. Roy. Soc. (A)*, Vol. 117, p. 417, 1928.
3. GILBARG, D. AND SERRIN, J., "Free Boundaries and Jets in the Theory of Cavitation," *J. of Math. and Phys.*, Vol. 29, No. 1, 1950.
4. RIABOUCHINSKY, D., "On Steady Fluid Motions with Free Surfaces," *Proc. London Math. Soc.*, Vol. 19 (2), p. 206, 1921.
5. KREISEL, G., "Cavitation with Finite Cavitation Numbers," *Admiralty Research Laboratory Report*, No. R1/H/36, Jan. 1946.
6. Roshko, A., "A New Hodograph for Free-Streamline Theory," *NACA TN 3168*, July 1954.
7. EPPLER, R., "Beiträge zu Theorie und Anwendung der un stetigen Strömungen," *Journal of Rational Mechanics and Analysis*, Vol. 3, No. 5, p. 591, 1954.
8. GUREVICH, M., "Some Remarks on Stationary Schemes for Cavitation Flow about a Flat Plate," *David Taylor Model Basin Translation No. 224*, 1948.
9. GILBARG, D. and ROCK, H. H., "On Two Theories of Plane Potential Flows with Finite Cavities," *Naval Ordnance Laboratory, Memorandum 8718*, August 1946.
10. GOLDSTEIN, S., "Modern Developments in Fluid Mechanics," *Oxford Press*, 1950.
11. FAGE, A. AND JOHANSEN, F. C., "On the Flow of Air Behind an Inclined Flat Plate of Infinite Span," *R and M No. 1104*, *British A.R.C.*, 1927.
12. PLESSET, M. S. AND PERRY, B., "On the Application of Free Streamline Theory to Cavity Flows," *Extrait des Mémoires sur la Mécanique des Fluides, offerts à M. D. Riabouchinsky a l'occasion de son Jubilé Scientifique, Ministère de l'Air*, 1954.
13. REICHARDT, H., "The Laws of Cavitation Bubbles at Axially Symmetrical Bodies in a Flow," *MAP Reports and Translations No. 766*, 1946.
14. MILNE-THOMSON, L. M., "Theoretical Hydrodynamics," *Macmillan Co.*, 1949.
15. LAMB, H., "Hydrodynamics," *Dover Publications*, New York, 1945.
16. LEVI-CIVITA, T., "Scie e leggi de resistenza," *Rend. Cir. Mat. Palermo*, 23, p. 1, 1907.
17. SCHLICHTING, H., "Boundary Layer Theory," *NACA TM No. 1218*, 1949.
18. PARKIN, B. R., "Experiments on Circular Arc and Flat Plate Hydrofoils in Noncavitating and in Full Cavity Flow, *California Institute of Technology, Hydrodynamics Laboratory Report* (in preparation).

CALIFORNIA INSTITUTE OF TECHNOLOGY  
PASADENA, CALIFORNIA

(Received September 19, 1955)